Materials Science Forum Vols. 556-557 (2007) pp 965-970
online at http://www.scientific.net

Online available since 2007/Sep/15

SiC-based Power Converters for High Temperature Applications

Leon M. Tolbert[1,2,a], Hui Zhang[1,b] , Madhu S. Chinthavali[2,c], Burak Ozpineci[2,d]

[1]The University of Tennessee, Electrical and Computer Engineering, Knoxville, Tennessee, USA

[2]Oak Ridge National Laboratory, National Transportation Research Center, Knoxville, TN, USA

[a]tolbert@utk.edu, [b]hzhang18@utk.edu, [c]chinthavalim@ornl.gov, [d]ozpinecib@ornl.gov

Keywords: converter, inverter, high temperature, hybrid electric vehicle

Abstract. As commercial-grade silicon carbide (SiC) power electronics devices become available, the application of these devices at higher temperatures or frequencies has gained interest. This paper contains temperature-dependent loss models for SiC diodes and JFETs and simulations for different power converters that are useful for predicting the efficiency of these converters. Additionally, tests to characterize the static and dynamic performance of some available devices are presented to give further insight into the advantages that might be gained from using SiC devices instead of Si devices for hybrid electric vehicle applications.

Introduction

Increasing demand for more efficient, higher power, and higher temperature operation of power converters has led to the development of wide bandgap semiconductor power electronic devices and in particular silicon carbide (SiC) power electronics. The high temperature operation capability of these devices increases the power density of converters incorporating them because of reduced thermal management and heat sink requirements that yield reduced weight and cost. To ultimately gain full advantage of SiC power electronics devices requires high temperature packaging techniques, gate drives, and passive components [1-4]. Device and system-level temperature-dependent loss models have been developed for transportation applications and utility applications to aid in gauging the impact that these new devices might have in terms of efficiency and heat sink requirements [5-7]. Device and system loss models for SiC diodes, JFETs, and MOSFETs have shown that they will become the devices of choice once issues such as fabrication and packaging of these devices are solved.

At present, SiC Schottky diodes are the only commercially available SiC devices. These diodes are used in several applications, and have proved to increase the system efficiency compared with Si device performance when used as antiparallel diodes in bridge converters [8-9]. Significant reduction in weight and size of SiC power converters with an increase in the efficiency is projected.

Some applications such as hybrid electric vehicles require that devices be able to handle extreme environments that include a wide range of operating temperatures (from -40ºC to 200ºC). In the following sections, models and experimental tests for the static and dynamic performance of some commercially available SiC Schottky diodes and experimental samples of SiC JFETs and MOSFETs in a wide temperature range will be presented.

Temperature Dependent Modeling of SiC Schottky Diodes

In this section, SiC Schottky diodes are characterized by both theoretical analysis and experiments. The models for static state (forward conduction) and dynamic state (reverse recovery) will be discussed.

Schottky Diode Static State. The structure of a SiC power Schottky diode and its equivalent circuit are shown in Fig. 1. V_{FB} is the voltage drop across the Schottky barrier; R_D is the resistance of the lightly doped drift region; R_S and R_C are the resistances of substrate and contact, respectively.

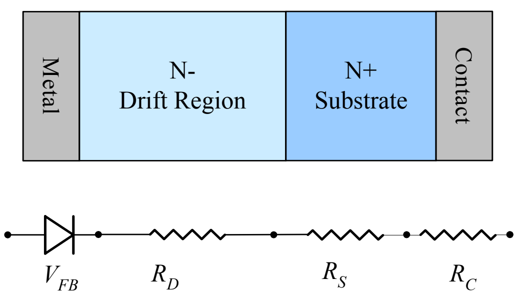

Fig. 1. (Above) Basic structure and equivalent circuit of Schottky power diodes.

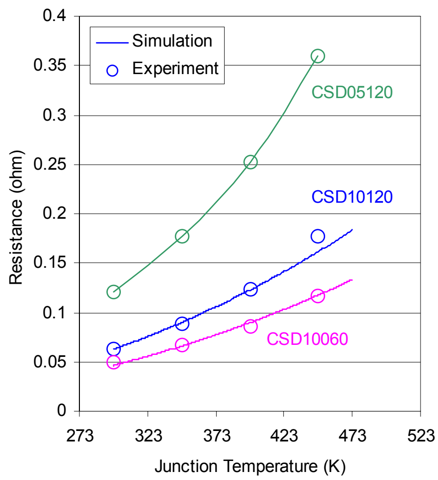

Fig. 2. (Right) On-state resistance of SiC Schottky diodes with respect to temperature (Cree).

In a SiC Schottky power diode, the thermionic emission process dominates in the transport of current across a metal *n*-type semiconductor contact [10]. Under the forward bias condition, the current flow across the Schottky barrier is given by

$$J_F = CT^2 e^{q(V_{FB}-\phi_B)/kT}, \tag{1}$$

where ϕ_B is the barrier height between the metal and *n*-type semiconductor, T is the absolute temperature, q is the charge of an electron, k is Boltzmann's constant, C is Richardson's constant, which is given by

$$C = \frac{4\pi m k^2 q}{h^3}, \tag{2}$$

where m is the effective mass of an electron, and h is Plank's constant [10]. For 4H-SiC, the theoretical value of Richardson's constant is 146 $A \cdot cm^{-2} \cdot K^{-2}$ [11].

Solving Eq. 1 for V_{FB}, and neglecting R_S and R_C (because they are usually small compared to R_D for power devices with breakdown voltages larger than 200 V), then the total voltage drop across a Schottky power diode can be expressed as

$$V_F = \phi_B + \frac{kT}{q}\ln\left(\frac{J_F}{CT^2}\right) + J_F R_D, \text{ where } R_D \text{ is given by } R_D = \frac{4V_B^2}{\varepsilon E_c^3 \mu_n}. \tag{3}$$

V_B is the breakdown voltage; E_c is the breakdown electrical field; μ_n is electron mobility, which is a function of doping density N_d, electrical field E, and temperature T in the depletion layer. μ_n can be expressed as

$$\mu_n = \frac{\mu_0}{\left[1+\left(\frac{\mu_0 E}{v_s}\right)^{\beta}\right]^{1/\beta}}, \quad \mu_0 = \mu_{\min} + \frac{\mu_{\max}-\mu_{\min}}{1+\left(N_{tot}/N_{ref}\right)^{\alpha}}, \quad v_s(T) = \frac{v_{\max,600K}}{1+0.8\cdot\exp\left(\frac{T}{600}\right)} \tag{4}$$

$$\mu_{\max} = A_{\mu\max} \times \left(\frac{T}{300}\right)^{-B_{\mu\max}}, \quad \mu_{\min} = A_{\mu\min} \times \left(\frac{T}{300}\right)^{-B_{\mu\min}}, \quad N_{ref} = A_{N_{ref}} \times \left(\frac{T}{300}\right). \tag{5}$$

Eqs. 3-5 give a comprehensive description of the static characteristics of SiC Schottky power diodes. The coefficients involved can be found in many papers, and only the breakdown voltage of the devices is needed to solve the equations [12]. Table 1 has a list of the parameters used to model the forward characteristic for a 1200V/10A 4H-SiC Schottky power diode.

Differentiation of Eq. 3 with respect to J_F yields the on-state specific resistance of a power Schottky diode:

$$R_{sp} = \frac{dV_F}{dJ_F} = \frac{kT}{q}\left(\frac{1}{J_F}\right) + R_D \,. \tag{6}$$

TABLE 1. PARAMETERS USED IN SIMULATION

Property	4H-SiC
Breakdown electric field, E_c (kV/cm)	2200
Relative dielectric constant, ε	10.1
Doping coefficient of μ, α	0.76
Electric field coefficient of μ, β	1
Coefficient of μ_{max}, $A_{\mu_{max}}$	950
Coefficient of μ_{max}, $B_{\mu_{max}}$	2.4
Coefficient of μ_{min}, $A_{\mu_{min}}$	40
Coefficient of μ_{min}, $B_{\mu_{min}}$	0.5
Coefficient of N_{ref}, $A_{N_{ref}}$	2×10^{17}
Maximum saturated velocity, $v_{s\,max}$ (cm/s)	4.77×10^{7}
Schottky barrier height, ϕ_B (eV)	1.25
Richardson's constant, A ($A\cdot cm^{-2}\cdot K^{-2}$)	146

Eq. 6 shows the dependence of the diode's on-state specific resistance to temperature and forward current. Moreover, as the forward current increases, the contribution of the first term in Eq. 6 becomes smaller and can be neglected. This means that the on-state resistance is nearly constant regardless of forward current and only changes with temperature at a relatively high current region. Most SiC power Schottky diodes operate in this region. Thus, it is reasonable to only consider drift region resistance R_D in system modeling. Correspondingly, the temperature dependence of the on-state resistance is determined by the change of μ_n with temperature. Fig. 2 compares simulation results to experimental results of several SiC Schottky diodes from Cree at different junction temperatures.

High Temperature Conduction Tests of SiC Schottky Diodes. Several 600 V, 75 A SiC Schottky diodes manufactured by Cree were packaged by the University of Arkansas for high temperature operation. These packaged diodes were placed with no heat sink in an environmental chamber with an ambient of 200ºC. The diodes were initially tested in the forward conducting state at various current levels as shown in Fig. 3. Fig. 3(b) shows the increase in forward voltage drop with the temperature increase. The diode ultimately failed short when the case temperature exceeded 550ºC with a forward current of 25 A.

Schottky Diode Dynamic State. Reverse recovery is the most important dynamic behavior of power Schottky diodes. Since there is no minority carrier injection in power Schottky diodes, the depletion layer capacitance determines their behavior during reverse recovery. When a reverse biased voltage V_R is applied to a power Schottky diode, the width of its depletion layer can be calculated from well-known device theory:

$$w_d = \sqrt{\frac{2\varepsilon(V_R + \phi_B)}{qN_d}} \,. \tag{7}$$

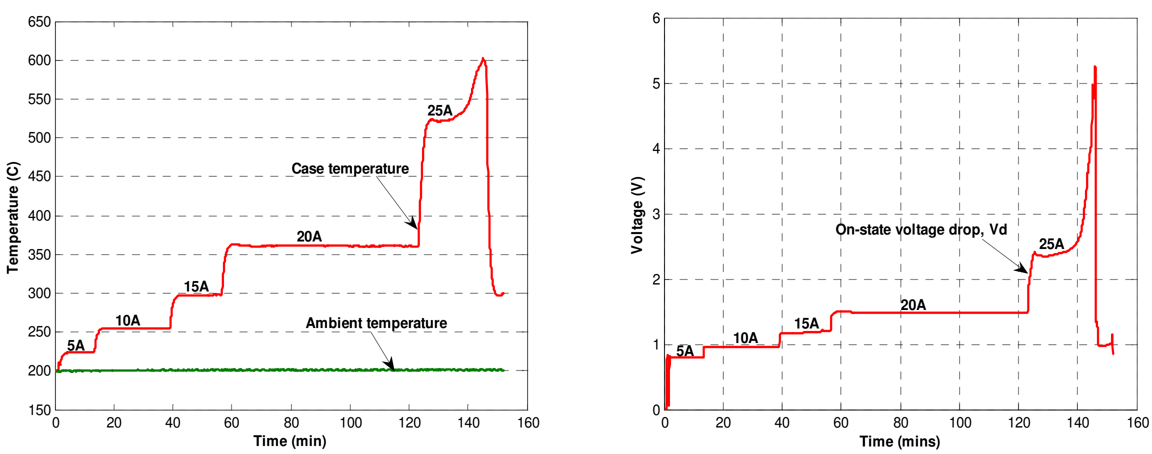

(a) (b)

Fig. 3. (a) Experimental case temperature of a 600 V, 75 A SiC Schottky diode as forward current is increased. (b) Forward voltage drop of diode as a function of temperature.

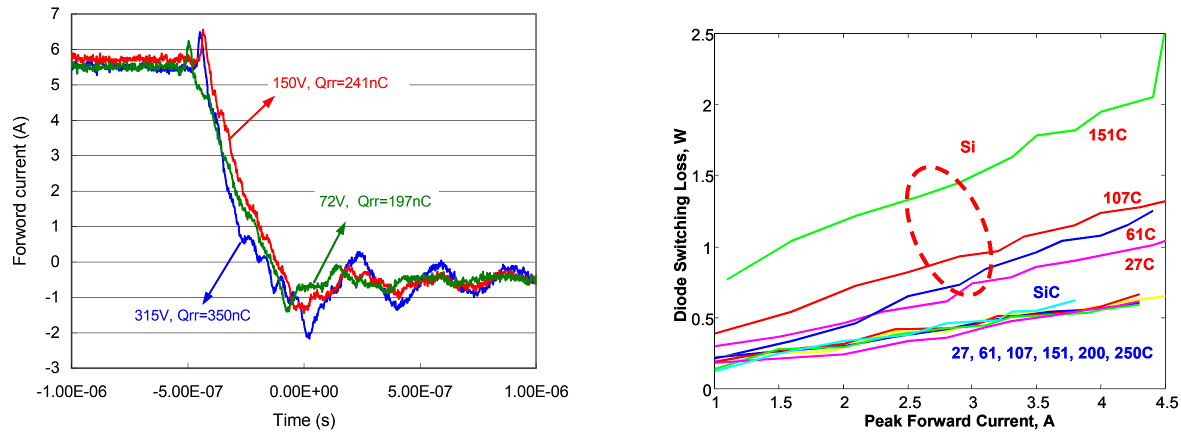

(a) (b)

Fig. 4. (a) Reverse recovery waveforms of the SiC Schottky diode. (b) Experimental Si and SiC peak reverse recovery current values at different temperatures.

Then, the specific depletion layer capacitance can be represented as

$$C_d = \frac{\varepsilon}{w_d} = \sqrt{\frac{qN_d\varepsilon}{2(V_R + \phi_B)}} \quad . \tag{8}$$

As shown by Eq. 8, C_d is a strong function of V_R, but is not affected by the current flowing through it. That is to say, the switching loss of a SiC Schottky diode mainly depends on the reverse voltage. Thus, in system modeling, it is reasonable to model the reverse recovery charge of SiC Schottky diodes as a function of their reverse voltage. Specifically, the reverse-recovery charge increases approximately linear with $V_R^{0.5}$, and the energy loss during this period increases linearly with $V_R^{1.5}$.

Switching Tests of a SiC Schottky Diode. A SiC Schottky diode (Cree CSD10120) was tested at different reverse voltages with the same forward current. The turn-off characteristics are shown in Fig. 4(a). As expected, the reverse-recovery charge increased as the reverse voltage increased, and the ratio of reverse-recovery charge at 315 V to that at 150 V is 1.452, which coincides with the square root of 315V/150V (1.449). In addition, if the slight changes of ε and ϕ_B with temperature are not considered, the reverse recovery behavior of SiC Schottky diodes will be the same at any temperature. This is also consistent with the test results shown in Fig. 4(b), where the peak reverse recovery current for a SiC diode was essentially constant for a temperature range of 27ºC to 250ºC. Thus, in system modeling, the influence of temperature on the reverse recovery characteristics of SiC Schottky diodes can be neglected.

SiC Power VJFET

Because a VJFET has an on-state resistance similar to that of a Schottky diode, Eq. 3 can also be used to model its on-state resistance while it is conducting. The switching loss model for a SiC VJFET is discussed in the following section when analyzing the loss in a power converter. Fig. 5(a) shows the I-V curves for a 1200 V, 10 A SiC JFET from SiCed for temperatures from -50ºC to 175ºC. As shown in Fig. 5(b), the on-state resistance increases with increasing temperature from 0.25 ohms at -50ºC to 0.60 ohms at 175ºC. Fig. 5(c) shows the switching losses for the SiC JFET as a function of temperature and forward current. This figure shows the switching losses decreased by approximately 25% when the JFETs were operated at a case temperature of 100ºC compared to 25ºC.

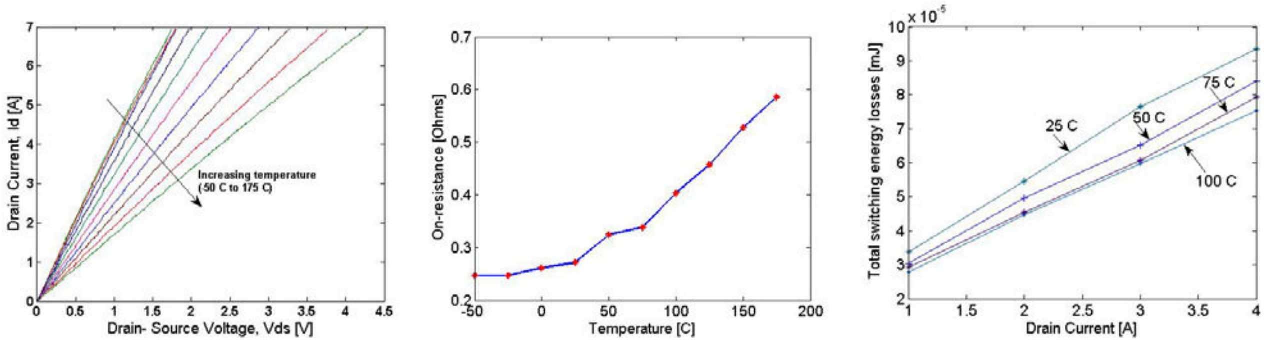

(a) (b) (c)

Fig. 5. (a) Experimental I-V curve for a 1200 V, 10 A SiC JFET for temperatures from -50ºC to 175ºC. (b) On-state resistance of JFET versus temperature. (c) Switching loss for JFET for temperature range from 25ºC to 100ºC.

Full-Bridge Converter Power Loss Model

A common converter found in traction applications and utility applications is a three-phase, full-bridge inverter [7, 11]. Converter loss models have three parts, namely single device loss models, converter power loss models, and thermal models as shown in Fig. 6. Single device models are the basis of the converter models, which describe device characteristics in both conduction and switching periods under different temperatures. The converter power loss models use an averaging technique to estimate the system power loss under a specific control strategy. Their inputs are device characteristics given by single device models and the system operation variables (inverter dc input voltage, ac output current, modulation index, and power factor) calculated by the model. Their outputs are the power losses of switches and diodes. These power losses are fed into the thermal models to get real-time junction temperatures of devices. At the same time, the temperatures are fed back to the single device models in order to update device characteristics. A thermal equivalent circuit model of the converter that includes the device, packaging, and heat sink has been developed to determine what temperature the devices in the converter will be for given ambient conditions and converter loss profile.

Fig. 7 shows the simulation results comparing a Si-based inverter with a SiC-based inverter for a battery charging and discharging application. Full details of the model can be found in [9]. The power loss savings of the SiC Schottky diode due to its inherent lower on-state resistance and better reverse recovery characteristics reduced the temperature rise of the SiC system dramatically when using the same heatsink and ambient temperature as the Si system. This resulted in lower losses in the SiC-based system and an efficiency greater than 99% for the SiC-based system compared to just more than 96% for the Si-based system as shown in Fig. 7(d).

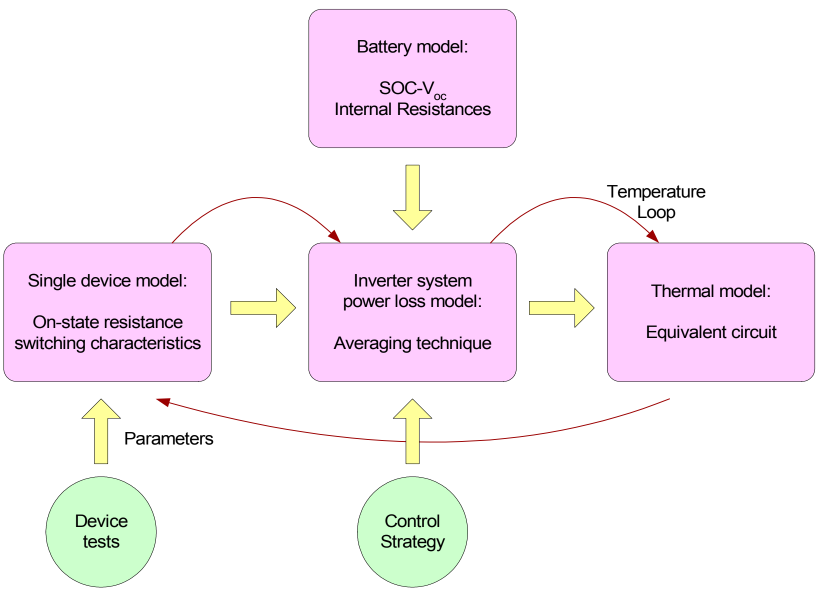

Fig. 6. Converter loss model for battery charging application.

Summary

This paper presented some models that can aid in determining the expected system benefits of using SiC devices in various applications. As SiC power electronics devices become more readily available, more research into the packaging and application of these devices will be needed to fully exploit their inherent high-temperature capabilities. Issues that will have to be addressed include high temperature gate drives, passive components, and packaging which includes the substrate, encapsulation, die attach, and connection.

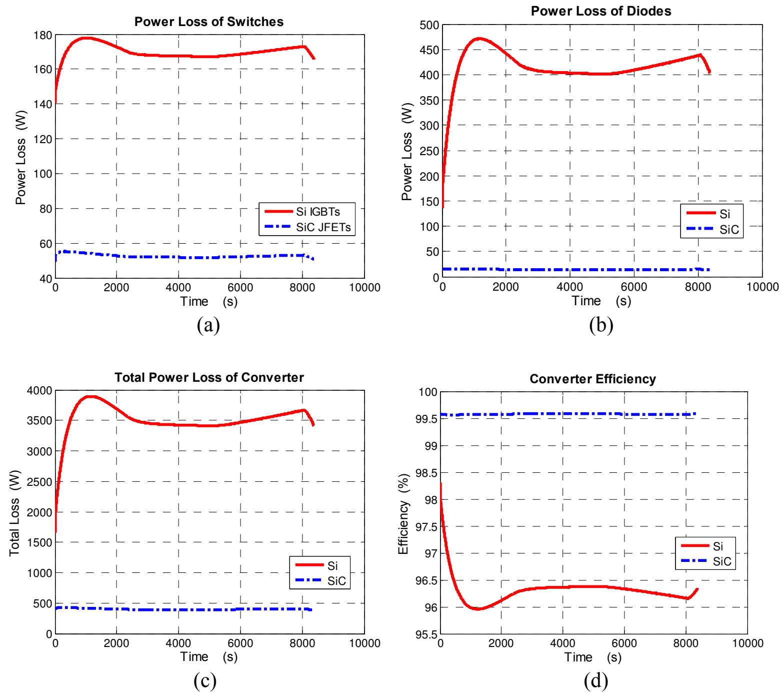

Fig. 7. (a) SiC JFET and Si IGBT device power losses during discharge (single device), (b) diode power losses, (c) converter system power losses, (d) converter efficiency.

Acknowledgment

The authors would like to thank Anant Agarwal and Jim Richmond of Cree for providing the SiC Schottky diodes. We also would like to thank Fred Barlow of the University of Idaho for the packaging of these devices while he was at the University of Arkansas.

References

[1] D. C. Hopkins, D. W. Kellerman, R. A. Wunderlich, C. Basaran, J. Gomez: IEEE Applied Power Electronics Conference (2006), p. 871.
[2] D. Katsis, B. Geil, T. Griffin, G. Koebke, S. Kaplan, G. Ovrebo, S. Bayne: IEEE Industry Application Society Annual Meeting (2005), p. 399.
[3] T. Funaki, J. C. Balda, J. Junghans, A. S. Kashyap, F. D. Barlow, H. A. Mantooth, T. Kimoto, T. Hikihara: IEEE Power Electronics Specialists Conference (2005), p. 2030.
[4] M. Chinthavali, B. Ozpineci, L. M. Tolbert: IEEE Applied Power Electronics Conference (2005), p. 322.
[5] H. Zhang, L. M. Tolbert, B. Ozpineci: IEEE Workshop on Computers in Power Electronics (2006), p. 199.
[6] L. M. Tolbert, B. Ozpineci, S. K. Islam, F. Z. Peng: SAE 2002 Transactions Journal of Passenger Cars - Electronic and Electrical Systems (2003), p. 765.
[7] H. Zhang, L. M. Tolbert, B. Ozpineci, M. Chinthavali: IEEE Industry Applications Society Annual Meeting (2006).
[8] B. Ozpineci, M. Chinthavali, A. Kashyap, L. M. Tolbert, A. Mantooth: IEEE Applied Power Electronics Conference (2006), p. 448.
[9] H. Zhang, L. M. Tolbert, B. Ozpineci, M. Chinthavali: IEEE Industry Applications Society Annual Meeting (2005), p. 2630.
[10] B. J. Baliga: *Modern Power Devices*, 1987.
[11] F. Roccaforte, S. Libertino, F. Giannazzo, C. Bongiorno, F. L. Via, and V. Raineri: Journal of Applied Physics, vol. 97 (2005).
[12] M. Roschke, F. Schwierz: IEEE Trans. on Electron Devices, vol. 48 (2001), p. 1442.